

Investigating the Use of Methane as an Alternative Fuel in Diesel Engines: A Numerical Approach

Mehmet Fatih Yaşar^{1*}, Gökhan Ergen¹ and İdris Cesur¹

0000-0001-7945-0239^{1*}, 0000-0003-4243-8409¹, 0000-0001-7487-5676¹

¹ Mechanical Engineering Department, Faculty of Technology, Sakarya University of Applied Sciences, Sakarya, 54100, Turkey

Abstract

The search for alternative fuels for diesel engines is being explored due to rising oil prices and increasing vehicle emissions. Due to its low cost and properties, natural gas is considered a suitable option for diesel engines. However, the costs required for research and misleading experimental setups can lead to time loss for researchers. Therefore, conducting computer simulations before experiments can reduce costs and provide faster access to desired data. Nonetheless, these simulations need to be compared with real experimental data. Hence, the study consists of two phases. In the first phase of the study, experiments were conducted with diesel fuel. Subsequently, a one-dimensional combustion model was developed in the AVL BOOST program. The established model was validated by comparing it with experimental data. Once the validated model was obtained, performance, emissions, and combustion analyses were carried out by adding different proportions of CH₄ (20%, 40%, 60%, and 80%) to diesel fuel using the model in AVL BOOST. As a result of the study, improvements in effective power and effective efficiency were achieved with the addition of varying proportions of CH₄ to the engine. Upon examining emitted exhaust emission values, it was observed that NO_x emissions increased while CO emissions decreased.

Keywords: Alternative fuel; Diesel engines; Performance; Emissions, Methane

Research Article

<https://doi.org/10.30939/ijastech..1333612>

Received 27.07.2023

Revised 24.08.2023

Accepted 08.09.2023

* Corresponding author

M. Fatih Yaşar

yasarm@subu.edu.tr

Address: Mechanical Engineering
Department, Faculty of Technology,
Sakarya University of Applied Sciences,
Sakarya, 54100, Turkey
Tel: +905058209094

1. Introduction

The need for energy is increasingly important in people's lives each day. This demand highlights various energy transformation processes and the environmental effects resulting from these processes. Engines are one of the most significant examples of these energy transformation processes. These machines, which convert a different form of energy into mechanical energy, produce various pollutant emissions during the energy conversion [1]. These emissions result in air pollution, which has serious effects on human health [2]–[4].

This situation has put automotive manufacturers into a conflicting but necessary situation to reduce emissions and ensure fuel economy. For this reason, researchers have begun to search for alternative fuels. The increasing use of diesel engines has accelerated the search for alternative fuel options. Various alternative fuel studies exist in international literature, dependent on countries technological and industrial developments and energy resources. For diesel engines, liquefied petroleum gas (LPG), natural gas, hydrogen, biodiesel, alcohol, and alcohol-derived fuels (methanol, ethanol, etc.) appear to be significant options [5].

In the case of using natural gas in engines, with the increase of the natural gas ratio at high loads, NO_x emissions decrease, but at low loads, it leads to higher CO and unburned hydrocarbon emissions [6]. Additionally, lower NO_x emissions can be obtained with dual fuel natural gas diesel fuel studies

compared to diesel fuel with injection timing [7]. The study conducted by Imran et al. found that the natural gas-based dual fuel caused a significant decrease in NO_x emissions compared to diesel [8].

In recent years, the use of methane in diesel engines has been the subject of significant research. Methane, available in various forms such as methane hydrates, natural gas, biogas, compressed natural gas, liquid natural gas, synthetic natural gas, and pipe natural gas, can be effectively used in diesel engines in dual-fuel mode with few modifications [9]. The high calorific value, abundant diffusion, and wide flammability limit of methane make it a suitable fuel for improving the performance of compression ignition engines in dual-fuel mode [9].

In addition to methane, alternative fuels, such as biodiesel derived from frying oil, have also been investigated. These fuels have the potential to reduce emissions of total hydrocarbons (THC) and carbon monoxide (CO) [10]. This suggests that methane and other alternative fuels can be effectively used in diesel engines.

Moreover, installing engines with different fuel types, such as CNG, on agricultural trucks has been proposed as a solution to the shortcomings of the diesel power unit [11]. Furthermore, using a turbocharger in a diesel power unit has been considered for engine modernization [12].

However, more research and development are needed to widely adopt methane and other alternative fuels. In particular,

further studies should be conducted on the current challenges and future perspectives of using methane in diesel engines [9].

Previous studies conducted with numerical methods include the following: In the study conducted by Wojs and colleagues, computer simulations performed with AVL BOOST showed that high heat could be obtained in the initial combustion stage with maximum pressure in the combustion chamber [13]. In the study by Saulius Stravinskas and colleagues, the AVL BOOST software examined the combustion characteristics of natural gas and diesel blends. The effect of the natural gas ratio on combustion was determined by changing the gas mass fraction in the fuel mixture, and it was shown that the use of methane gas improves performance and emission parameters [14]. R. G. Papagiannakis and Hountalas, [15] investigated the effects of using natural gas and diesel fuel in a dual-fuel diesel engine on engine performance and emission characteristics. They observed a decrease in cylinder pressure values and specific fuel consumption values, as well as an increase in combustion duration and total heat release values due to the use of natural gas as a dual fuel. Additionally, they identified an increase in CO and HC emissions and a decrease in NO_x and particulate matter emissions. Nwafor, [16] examined the impact of natural gas usage in a single-cylinder dual-fuel diesel engine. In their study, they explored the effects of varying natural gas proportions at different loads on engine performance and emission characteristics. They found that as the load increased, there was an increase in cylinder pressure and total heat release, while ignition delay, combustion duration, and specific fuel consumption decreased. With increasing load, they observed a reduction in soot, HC, and CO emissions, and an increase in NO emissions. Abd-Alla et al. [17] investigated the influence of the advance angle when using methane gas, the main component of natural gas, in a dual-fuel diesel engine, on HC, CO, NO_x emissions, and effective efficiency. Their study revealed that advancing the injection timing improved effective efficiency, attributed to the higher pressure and temperature conditions inside the cylinder. They noted that advancing the timing led to an increase in NO_x emissions and a decrease in CO and HC emissions.

In this study, the design of a single-cylinder diesel engine was modeled one-dimensionally through the AVL Boost program. The results of the experimental studies carried out with the model created were close. Then, keeping the total amount of fuel in the cylinder constant, the diesel fuel ratio was reduced, and methane was used at specific fractions (%20, %40, %60, %80) along with diesel fuel. The engine performance and emission results were examined through the obtained parameters.

2. Material Method

2.1. Experimental Study

In the first phase of the study, the performance and exhaust emission values of a Superstar brand, direct injection, and water-cooled diesel engine were measured under full load conditions. The technical specifications of the diesel engine used in the experiments are provided in Table 1.

The specifications of the experimental engine are given in Table 1.

In the study, a hydraulic dynamometer was used to measure the performance parameters. An S-type load cell with a sensitivity of 0.01 kg was employed to determine the engine

torque. For measuring the fuel consumption of the engine in the experiments, a gravimetric measurement method was used, with a measurement precision of 0.01 grams.

Table 1. Specifications of the experimental engine

Operating mode	Four-stroke, direct injection, water-cooled
Number of cylinders	1
Cylinder diameter	108 mm
Stroke	100 mm
Compression ratio	1:17
Engine power	11.7 kW (16 HP)
Specific fuel consumption	253.25 g/kW.h
Injector pressure	175 kgf/cm ²
Injection start	28° Crankshaft Angle
Intake valve opening	15° before Top Dead Center (TDC)
Exhaust valve closing	15° after Top Dead Center (TDC)

For cylinder pressure measurements, a Kistler 6061 B brand cylinder pressure measurement sensor and a Kistler 5011 B model charge amplifier were utilized. The MRU brand exhaust emission measurement device was employed for emission measurements in the experiments. NiCr-Ni type thermocouples were used at specific points on the test bench for temperature measurements.

The measurement values and uncertainties arising from measurement instruments in the experiments are provided in Table 2.

Table 2. Systematic and random uncertainties

Parameters	Systematic uncertainties
Load, N	0,1
Time, s	0,1
Temperature, °C	1
Fuel consumption, g	0,01
NO _x , ppm	%5
CO, %	%5
Parameters	Total uncertainties,%
Specific fuel consumption, g/kWh	1,4
Torque, Nm	1,2
Effective efficiency, %	1,4

2.2. Theoretical Study

In the second phase of the study, a zero-dimensional combustion model was established in the AVL BOOST program for a direct injection and naturally aspirated engine. The results obtained from the program will be presented in comparison with the results obtained from the experimental study for validation purposes.

In engine design, using computer-aided optimization tools is a common approach. These tools aim to determine the combinations of optimal design variables that minimize or maximize the specified objective functions, offering ease of use [18].

The AVL Boost program can be used to create one-dimensional models. One-dimensional equations are used for fluid dynamics calculations, and parameters such as temperature, pressure, and emissions can be calculated through this program. Suppose the dynamics of two or three-dimensional parts are to be calculated. In that case, the parameters obtained from the AVL Boost interface can be added to the AVL FIRE interface for a more detailed analysis [19].

Recently, the use of machine learning-based surrogate models for computational fluid dynamics (CFD) simulations is seen as a promising technique for reducing the computational cost in engine design optimization [19]. This technique has been combined with a vehicle dynamics model within an integrated user function framework in a Simulink® environment. In this context, the 1D engine model was used with a very coarse mesh providing a high acceleration factor to achieve the best simulation performance.

Basic equilibrium equations

The thermodynamic balance within a cylinder is calculated by the first law of thermodynamics, as expressed in the following formula:

$$\frac{d(m_c \cdot u)}{d\alpha} = -p_c \cdot \frac{dV}{d\alpha} + \frac{dQ_F}{d\alpha} - \sum \frac{dQ_w}{d\alpha} - h_{BB} \cdot \frac{dm_{BB}}{d\alpha} + \sum \frac{dm_i}{d\alpha} \cdot h_i - \sum \frac{dm_e}{d\alpha} \cdot h - q_{ev} \cdot f \cdot \frac{dm_{ev}}{dt} \tag{1}$$

The incoming and outgoing masses calculate the total mass change within the cylinder:

$$\frac{dm_c}{d\alpha} = \sum \frac{dm_i}{d\alpha} - \sum \frac{dm_e}{d\alpha} - \frac{dm_{BB}}{d\alpha} + \frac{dm_{ev}}{dt} \tag{2}$$

In these equations, $\frac{D(m_c \cdot u)}{d\alpha}$ represents the change in energy within the cylinder, $-p_c \cdot \frac{dV}{d\alpha}$ represents the work done by the piston, $\frac{dQ_F}{d\alpha}$ represents the heat provided by the fuel, $\sum \frac{dQ_w}{d\alpha}$ represents heat losses from the wall, $h_{BB} \cdot \frac{dm_{BB}}{d\alpha}$ represents the enthalpy flow due to blow-by, m_c represents the total mass within the cylinder, u represents the specific internal energy, p_c represents the pressure within the cylinder, V represents the instantaneous volume of the cylinder, Q_f represents the energy of the fuel, Q_w represents the heat loss to the wall, α represents the crank angle, h_{BB} represents the blow-by enthalpy, $\frac{dm_{bb}}{d\alpha}$ represents the blow-by flow rate, dm_i represents the mass entering the cylinder, dm_e represents the mass exiting the cylinder, h_i represents the enthalpy of the mass entering the cylinder, h_e represents the enthalpy of the mass exiting the cylinder, q_{ev} represents the heat of vaporization of the fuel, f represents the ratio of the fuel that vaporizes within the cylinder and m_{ev} represents the mass of the vaporized fuel.

According to the first law of thermodynamics, the energy change of the cycle is equal to the sum of the work done by the piston, the heat input provided by the fuel, the heat loss to the walls, and the energy loss due to blow-by [20].

Once the temperature within the cylinder is known for each crank angle, the pressure within the cylinder can be calculated using the ideal gas equation:

$$p_c = \frac{1}{V} \cdot m_c \cdot R_o \cdot T_c \tag{3}$$

Heat transfer model

The heat transfer value on the cylinder wall at any crank angle θ , for an engine operating at N engine speed, is expressed as:

$$\frac{\partial Q_w}{\partial \theta} = h_g(\theta)A(\theta)(T_g(\theta) - T_w)/(2\pi N) \tag{4}$$

P_r and V_r represent the pressure and volume values concerning the reference point, respectively. γ is the adiabatic index (ratio of specific heats) c_p/c_v . $A(\theta)$ and $V(\theta)$ represent

the wall area and total combustion chamber volume at that crank angle, respectively. $T_g(\theta)$ is the gas temperature inside the cylinder, and T_w is the wall temperature. $h_g(\theta)$ denotes the heat transfer coefficient.

The widely accepted Woschni model can be used to calculate the instantaneous heat transfer coefficient [21], [22]

$$h_g = 127.9D^{(-0.2)} \cdot P^{0.8} \cdot [T_g]^{(-0.53)} \cdot [C_1 V_p + C_2 \frac{V_s T_r}{p_r V_r} (p - p_m)]^{0.8} \tag{5}$$

Here P ve T represents the instantaneous pressure and temperature, respectively, D is the combustion chamber diameter, and V_p is the piston mean velocity. T_r , p_r , and V_r represent any reference point's temperature, pressure, and volume values. p and p_m indicate the ignition and compression end pressures, respectively. C_1 and C_2 are constant coefficients depending on the engine speed.

For the exhaust phase: $C_1 = 6.18, C_2 = 0$

For the compression phase: $C_1 = 2.28, C_2 = 0$

For the ignition and combustion phase: $C_1 = 2.28, C_2 = 0.00324$

To calculate the heat transfer in the manifolds, the modified Zaph heat transfer model can be used [23].

Mixture Controlled Combustion Model

For direct-injection compression-ignition engines, a model has been developed. Mixture-controlled combustion utilizes the heat release model, followed by the calculation of parameters such as ignition delay, which is crucial for the Wiebe function [24].

$$\frac{dQ_{MCC}}{d\alpha} = C_{Comb} \cdot f_1(m_F, Q_{MCC}) \cdot f_2(k, V) \tag{6}$$

Furthermore,

$$f_1(m_F, Q) = \left(m_F - \frac{Q_{MCC}}{LHV}\right) \cdot (W_{Oxygen,available})^{C_{EGR}}$$

$$f_2(k, V) = C_{Rate} \cdot \frac{\sqrt{k}}{\sqrt[3]{V}} \tag{7}$$

In the above equations, Q_{MCC} represents the total released heat C_{comb} is the combustion rate constant, C_{rate} is the mixing rate constant, k is the local turbulence kinetic energy density, m_f denotes the actual fuel evaporation mass, LHV is the lower heating value, V is the volume at crank angle $\alpha_{Oxygen,available}$, is the oxygen mass fraction, C_{EGR} is the EGR constant.

Conservation Equations for Kinetic Energy Possessed by Fuels

For fuel jets, the equations are:

$$\frac{dE_{kin}}{dt} = 0.5 \cdot C_{turb} \cdot m_f \cdot v_f^2 - C_{Diss} \cdot E_{kin}^{1.5}$$

$$k = \frac{E_{kin}}{m_{F,I}(1+\lambda_{Diff}m_{stoich})} \tag{8}$$

In the above equations, E_{kin} represents the jet kinetic energy, C_{turb} is the turbulence energy production coefficient, C_{Diss} is the dissipation constant, $m_{F,I}$ is the dissipation constant, $v_f = \frac{m_f}{\rho_F \mu A}$ is the injection velocity, μ is the injector hole diameter, ρ_F

is the fuel density, n is the fuel density, $m_{ostrich}$ is the stoichiometric air mass, λ_{diff} is the air excess ratio for diffusion combustion, and t represents time.

Ignition delay

Ignition delay refers to the time between fuel injection and the onset of combustion. The combustion process occurs when the fuel-air mixture is adequately premixed, and the thermodynamic and chemical properties are suitable [25]. For diesel engines, ignition delay depends on the chemical properties of the fuel and the characteristics related to fluid mechanics, such as atomization, vaporization, and mixing. Increasing cylinder pressure and temperature shorten the ignition delay period [31].

Hardenberg and Hase (1979) proposed a widely accepted equation for ignition delay [28]:

$$\tau_{id} = (0.36 + 0.22\overline{U}_p) \exp \left[E_A \left(\frac{1}{R_u T} - \frac{1}{17.190} \right) \left(\frac{21.2}{P-12.4} \right)^{0.63} \right] \quad (9)$$

where E_A is calculated as:

$$E_A = \frac{618.840}{CN+25} \quad (10)$$

Here, τ_{id} represents the ignition delay time (deg), \overline{U}_p is the average piston velocity (m/s), R_u is the gas constant (8.314), and r is the compression ratio.

Premix combustion model

A classical Wiebe function is used for premixed combustion [29]. Ghojel (2010) recently reviewed the Wiebe function [30].

$$\frac{\left(\frac{dQ_{PMC}}{Q_{PMC}} \right)}{d\alpha} = \frac{a}{\Delta\alpha_c} \cdot (m + 1) \cdot y^m \cdot e^{-a \cdot y^{(m+1)}} \quad (11)$$

$$y = \frac{\alpha - \alpha_{id}}{\Delta\alpha_c} \quad (12)$$

In the above equation, $Q_{PMC} = m_{fuel, id} \cdot C_{PMC}$ represents the heat contribution from premixed combustion, $\alpha_{fuel, id}$ is the amount of fuel sprayed during the ignition delay C_{PMC} is the premixed combustion parameter, $\Delta\alpha_c = \tau_{id} \cdot C_{PMC-Dur}$ is the premixed duration in degrees $C_{PMC-Dur}$ is the premixed duration factor, $m = 2$ is the form factor, $\alpha = 6.9$ is the wiebe parameter.

2.3. Chemical Kinetics

NOx Formation Model

The following 6 reactions (based on the well-known Zeldovich mechanism) are taken into account [27]: (Table 3)

Table 3. Zeldovich mechanism

	Stoichiometry	Rate
R1	$N_2 + O = NO + N$	$k_i = k_{0,i} \cdot T^a \cdot e^{\left(\frac{-T A_i}{T} \right)}$
R2	$O_2 + N = NO + O$	$r_1 = k_1 \cdot c_{N_2} \cdot c_O$
R3	$N + OH = NO + H$	$r_3 = k_3 \cdot c_{OH} \cdot c_N \cdot c_H$
R4	$N_2O + O = NO + NO$	$r_4 = k_4 \cdot c_{N_2O} \cdot c_O$
R5	$O_2 + N_2 = N_2O + O$	$r_5 = k_5 \cdot c_{O_2} \cdot c_{N_2}$
R6	$OH + N_2 = N_2O + H$	$r_6 = k_2 \cdot c_{OH} \cdot c_{N_2}$

CO Formation model

The CO formation model implemented in BOOST™ is based on Onorati et al.[26]. The following two reactions are taken into account: (Table 4)

Table 4. CO formation model

	Stoichiometry	Rate
R1	$CO + OH = CO_2 + H$	$r_1 = 6.76 \cdot 10^{10} \cdot e^{\left(\frac{T}{11702.0} \right)} \cdot c_{CO} \cdot c_{OH}$
R2	$CO + O_2 = CO_2 + O$	$r_2 = 2.51 \cdot 10^{12} \cdot e^{\left(\frac{-24055.0}{T} \right)} \cdot c_{CO} \cdot c_{O_2}$

3. Simulation of The Engine Cycle

3.1. Creation of the single-cylinder model

A model of the cycle can be created using AVL Boost. As seen in Figure 1, this is the interface of BOOST. After adding the engine components, they can be interconnected with pipes. These elements, associated with each other and the boundary conditions through the pipes, are used for engine simulation. It's as if you're building a virtual engine, piece by piece, to simulate its operation.

Here, SB1, C1, E1, and SB2 represent the input boundary condition, the cylinder, the engine used in the cycle, and the output boundary condition, respectively. Those starting with MP represent measurement points, and CAT1 denotes the catalyst.

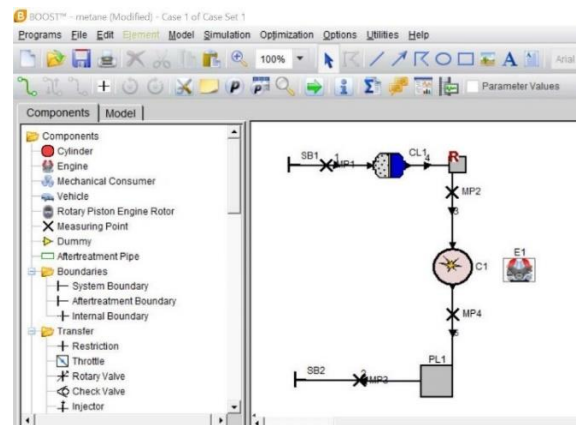


Fig. 1. AVL BOOST interface.

The fuel or dual fuel system to be used in the simulation can be set with the Simulation Control button. Additionally, this section has the capability to estimate the degree of noise.

3.2. Creation of the Theoretical Model from the Experimental Engine

A numerical analysis has been conducted through the AVL BOOST system. This process, visualized in Figure 1, has been achieved using the values specified in Table 1. These values, along with data obtained from the experimental engine, have been utilized to optimize a theoretical model.

The in-cylinder pressure graphs were analyzed at speeds of 1600 and 2400 revolutions per minute. This analysis played a critical role in the optimization of simulation inputs. Air excess coefficient (HFK)-(λ) was used to calculate the in-cylinder load for each revolution.

The start and end times of the injector have been included in the modeling. The geometry and characteristics of the injector - its diameter, spray pressure, spray timing, and number of holes - have a decisive effect on the in-cylinder pressure. Therefore, these features of the experimental engine have been thoroughly examined and included in the simulation.

Friction losses were among the data inputs of the theoretical engine, and these data were compared with the power obtained from the experimental engine. The heat transfer model was added to the modeling for the execution of emission calculations. The simulation engine was tested between 1200 and 2400 revolutions and the resulting emission values were examined.

In the final stage, the calculated parameters and coefficients were reused in the simulation with adding methane. In this process, where the coefficients were kept constant, methane was added to the fuel in certain proportions, and the results were analyzed in detail.

4. Research Findings and Discussion

In this section, the results of the conducted studies have been analyzed. Experimental and simulation data were compared and interpreted in the first part. In-cylinder pressure, engine power, engine torque, HFK, the flow rate of air drawn from the intake manifold, and CO and NO_x parameters have been examined in graphs according to engine speed in each subsection. After the optimization process, the effects of methane gas ratios as an alternative fuel were examined in the second part. Comparison of Experimental and Theoretical Results

According to the experimental results obtained from the diesel engine used in Table 5, the percentage error of the simulation results is provided.

4.1. Comparison of in-cylinder pressure graphs

Figure 2 presents the in-cylinder pressure graph obtained both experimentally and theoretically. The pressure graph was derived under full load conditions of our engine, using standard diesel fuel at 1600 rpm. Upon examining the figure, it's evident that the experimental data and theoretical data yield close values. The maximum pressure value for 1600 rpm on both data graphs occurs at the Top Dead Center (TDC) value, seen as 8° . In the experimental engine, a pressure drop occurs at -5° TDC due to the diesel fuel drawing heat from the environment [27].

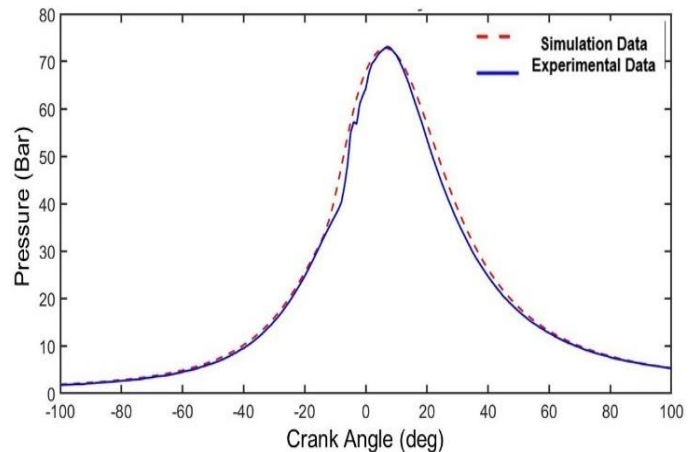


Fig. 2. Comparison of cylinder pressure at 1600 rpm between experimental and simulation data

Figure 3 displays the heat release rate obtained both experimentally and theoretically. Upon examination, the experimental and theoretical results yield close values. As a result of the study, it is understood that the theoretical model operates in accordance with the experimental data.

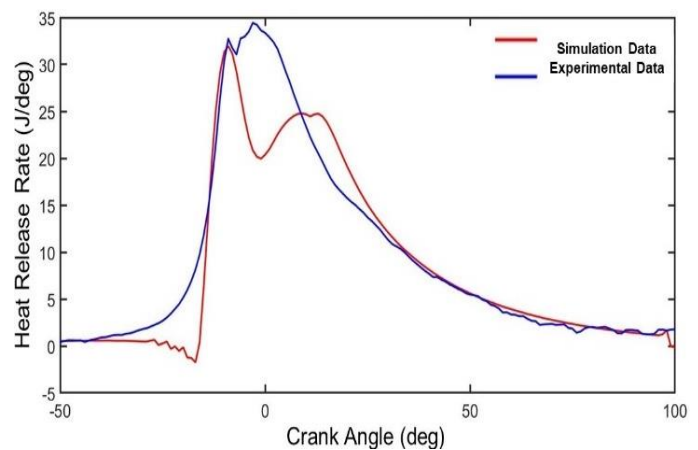


Fig. 3. Comparison of heat release rates at 1600 rpm between experimental and simulation data

Figure 4 shows the experimental and theoretical data obtained at the revolution where the engine's maximum power is given. Upon examining the graph, fluctuations in pressure data are observed at the values where maximum pressure occurs. The reason for these fluctuations is the increased tendency for knocking with increasing engine speed and ignition delay as TDC with increasing speed. The theoretical model sees the maximum pressure point as 5° TDC from the top dead center. Additionally, the amount of heat dissipation obtained with diesel fuel at the revolution at maximum power is given in Figure 5. Upon examination, the theoretical and experimental results remain within close values. Depending on the pressure value, fluctuations in heat dissipation values have also been observed in diesel fuel. The results examined indicate that the theoretical model is compatible with the experimental results [28].

Table 5. Percentage differences of simulation data compared to experimental data

Speed	Power, kW	Torque, Nm	HFK (λ)	m_{hava} , kg/h	CO_2 , %	O_2 , %	NO_x , ppm	CO , %
Percentage differences A(%)								
1200	0	0.05	0.36	0.17	2.1	2.95	0	10.16
1400	0.25	0.3	0.26	0.13	2.1	2.8	0	1.55
1600	0.08	0.13	0.24	0.34	1.32	1.18	0	0.55
1800	0.09	0.04	0.03	0.23	1.45	1.16	0	1.48
2000	0.32	0.37	0.17	1.55	1.79	4.78	0	1.76
2200	0.38	0.33	0.45	2.91	1.45	9.26	0	0.78
2400	0.04	0.09	0.46	0.75	2.41	10.92	0	0.57
Average	0.16	0.19	0.28	0.86	1.8	4.72	0	2.4

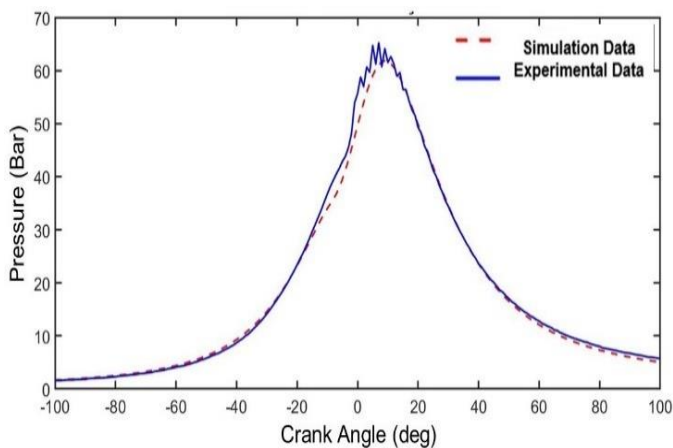


Fig. 4. Comparison of cylinder pressure at 2400 rpm between experimental and simulation data.

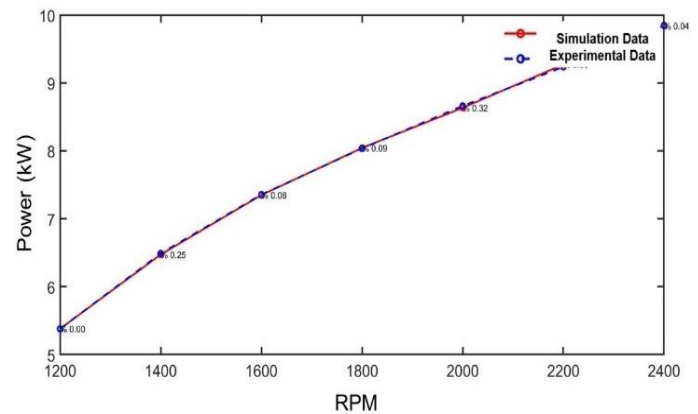


Fig. 6. Comparison of engine power at various engine speeds between experimental and simulation data

Figure 7 presents a comparative graph of the engine torque graph obtained experimentally from diesel fuel and the torque graph calculated with the theoretical model. It is seen that the results of the theoretical model are close to the experimental study conducted.

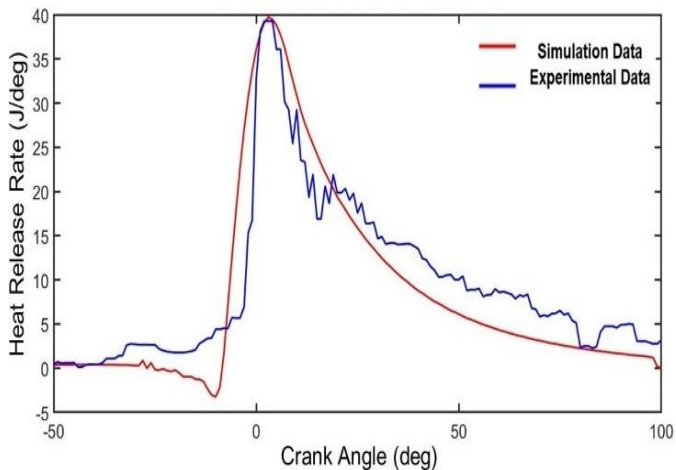


Fig. 5. Comparison of heat release rates at 2400 rpm between experimental and simulation data.

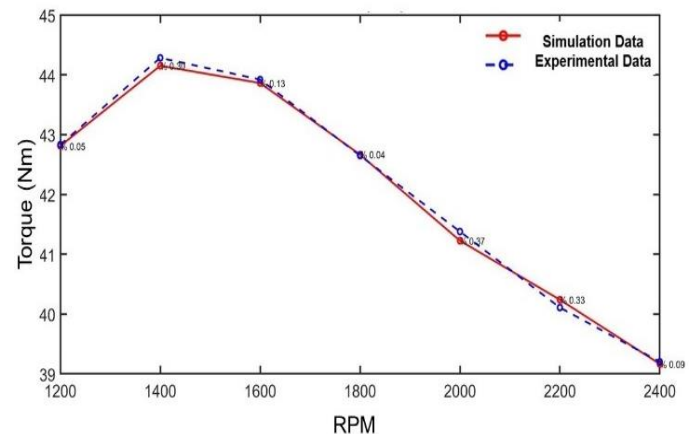


Fig. 7. Comparison of engine torque at various engine speeds between experimental and simulation data

4.2. Comparison of engine power and torque

Figure 6 presents a comparative graph of the effective power graph obtained experimentally from diesel fuel and the effective power graph calculated with the theoretical model. Upon examination, it is seen that the experimental results are close to the theoretical results. This suggests that the established model is suitable for experimental study. The added friction loss rates for the theoretical model support these results. The error rate has been calculated as less than 0.5%.

4.3. Comparison of experiment and theoretical model air redundancy coefficient λ

In Figure 8, the Lambda changes according to the experimental and theoretical diesel fuel results are given comparatively. Upon examination, it is seen that the HFK value of the engine is within close values of the experimental and theoretical results.

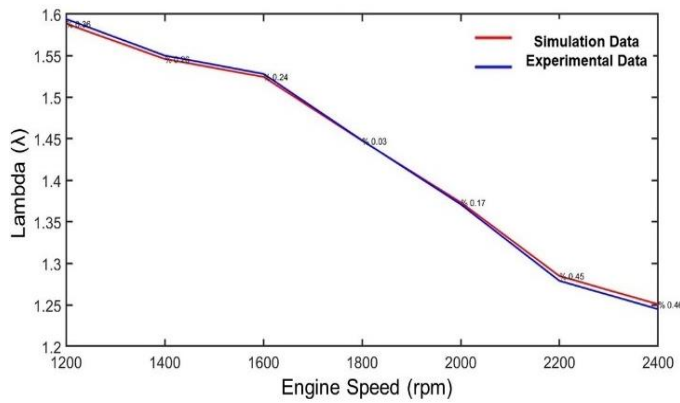


Fig. 8. Comparison of Lambda at various engine speeds between experimental and simulation data

4.4. Comparison of real and theoretical model CO

Based on experimental and theoretical results, the comparative CO emission values for diesel fuel are presented in Figure 9. Upon examination, it is observed that the CO emission value of the engine is within close values of the experimental and theoretical results. If the fuel-air mixture does not contain enough air, a deficient oxygen environment forms during combustion, and the carbon in the fuel remains as CO instead of fully converting to CO_2 . Carbon monoxide (CO) formation decreases with an increase in the air excess coefficient. By examining Figures 8 and 9, it can be observed that the amount of CO increases as the HFK number decreases.

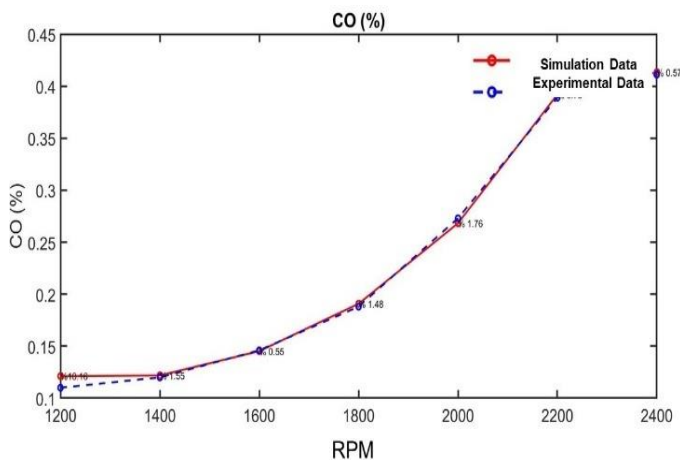


Fig. 9. Comparison of CO emissions at various engine speeds between experimental and simulation data

4.5. Comparison of NOx emissions

The formation of nitrogen oxides is influenced by factors such as temperature and the air excess coefficient. As a result of the nonlinear effect of these factors, it is observed that nitrogen oxides form in different amounts at different temperatures. Nitrogen oxides emerge when nitrogen in the air reacts with oxygen at high temperatures resulting from combustion under normal conditions. The NOx values obtained experimentally and theoretically are seen in Figure 10. Upon examining the graph, theoretical results consistent with experimental data have emerged [31].

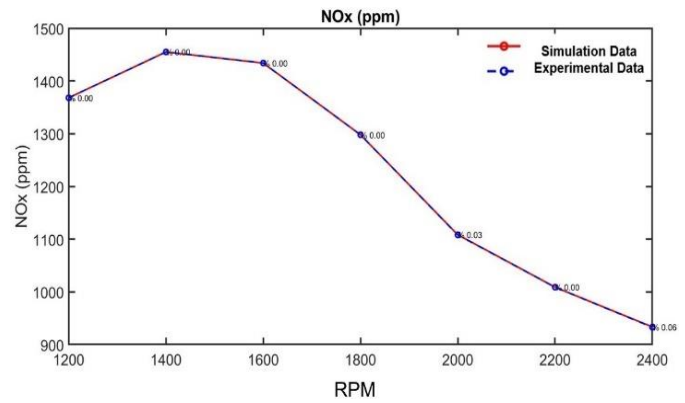


Fig. 10. Comparison of NOx emissions at various engine speeds between experimental and simulation data

5. The Effect of Dual Fuel (Diesel–Methane) Use on Performance and Emissions

In the first stage of the study, the theoretical model data set up in the AVL program is given comparatively with experimental data. When the results of the theoretical model are compared with the experimental results, the accuracy of the established model has been ensured. In the study's second stage, methane addition's effects on engine performance and exhaust emissions were theoretically examined in the confirmed theoretical model.

5.1. In-cylinder pressure

The effect of adding different proportions of methane to diesel fuel on the pressure change for the cylinder is theoretically examined in Figure 11. Upon examination, the in-cylinder pressure value increases as the addition of methane to diesel fuel increases. The maximum pressure is low at low speeds because the fuel mixture increases ignition delay. Methane, which has a high cetane number, reduces the cetane number of the mixture as it mixes with diesel fuel, and the ignition start is later. At high speeds, the high temperature and pressure bring the ignition start to almost the same crankshaft angle as pure diesel fuel. The increase in the in-cylinder pressure value with the addition of methane is because methane's lower heating value is higher than that of diesel fuel [34]. In their study, Vávra and others (2017) showed that the increase in natural gas fractions increases in-cylinder pressure, and power increases by 11% at low loads [35]. These results support that the in-cylinder pressure and power are proportional to the filling amount in the combustion chamber and that high-pressure levels can be reached in the cylinder according to the filling rate [8].

At 1400 rpm where maximum torque is attained, the peak pressures varied based on the percentage of methane addition to pure diesel. A 20% methane addition led to a 1.01% increase, reaching 73.62 bar, while increments of 40%, 60%, and 80% in methane concentration led to pressures of 74.34 bar, 75.08 bar, and 75.84 bar, respectively.

In contrast, at 2400 rpm where maximum power is generated, the peak pressures demonstrated a different trend. For a 20% methane supplement, there was a 1.31% elevation in pressure, registering 63.83 bar. This rose to 64.70 bar, 65.58 bar, and 66.29 bar for methane increments of 40%, 60%, and 80%, respectively.

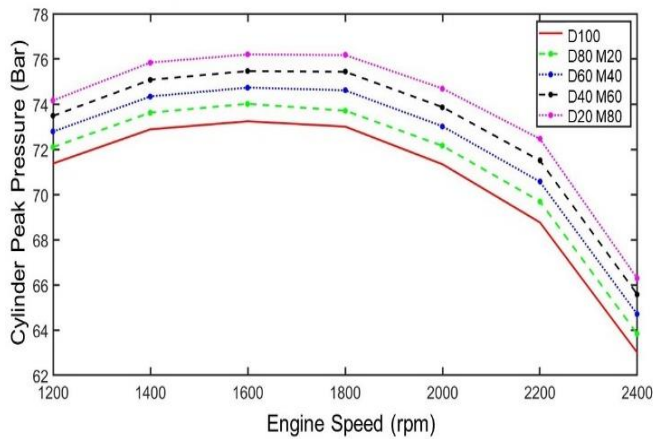


Fig. 11. Variation of Cylinder Peak Pressure with Different Fuel Compositions and Engine Speeds.

5.2. Engine power

The effect of adding different proportions of methane to diesel fuel on effective power is theoretically examined in Figure 12. Upon examination, as the addition of methane to diesel fuel increases, it causes increases in effective power at all revolutions. Maximum effective power was obtained with an 80% methane addition. The reason for the increases in effective power with the addition of methane is that the increase in in-cylinder pressure value with methane contribution causes increases in effective power.

Delving into the engine power at 1400 rpm, a 20% methane addition produced a power of 6.65 kW, marking a 3.13% difference from pure diesel. With the increase in methane concentration to 40%, 60%, and 80%, engine powers of 6.85 kW, 7.04 kW, and 7.24 kW were observed.

In the scenario of 2400 rpm, the engine power statistics again shifted. 3.51% difference equating to 10.11 kW was noted with 20% methane. The values escalated to 10.44 kW, 10.76 kW, and 11.09 kW with methane contributions of 40%, 60%, and 80%

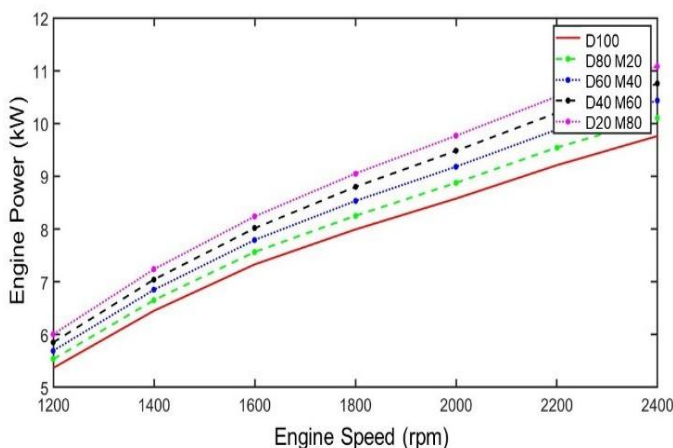


Fig. 12. Variation of engine power with different fuel compositions and engine speeds

5.3. Specific fuel consumption

The specific fuel consumption values obtained as a result of adding different proportions of methane to diesel fuel are seen in Figure 13. Upon examination, decreases in specific fuel consumption are seen in all methane additions. The reason for the decrease in specific fuel consumption is that the mixture fuel has more energy content than diesel fuel. In this way, less fuel

can obtain more power [16]. The increase in engine speed has caused the values of pressure and temperature inside the cylinder to increase. The increase in in-cylinder temperature has shortened ignition delay and combustion time. This effect improves combustion formation and improves specific fuel consumption compared to single fuel use [32]. This effect, which occurs significantly under high load, improves combustion formation and improves specific fuel consumption compared to single fuel use. Also, the lower heating value of methane gas being higher than diesel fuel allows similar performance values to be reached with less natural gas use with diesel [36].

Specific fuel consumption at 1400 rpm displayed an intriguing pattern. A 20% methane admixture showed a 3.09% deviation, amounting to 232.28 g/kWh. With the progressive increase in methane 40%, 60%, and 80% the values decreased to 225.52 g/kWh, 219.22 g/kWh, and 213.28 g/kWh respectively.

At the heightened speed of 2400 rpm, specific fuel consumption with a 20% methane boost showed a 3.30% difference 261.91 g/kWh. As methane concentration grew to 40%, 60%, and 80%, the values altered to 253.84 g/kWh, 246.40 g/kWh, and 239.40 g/kWh.

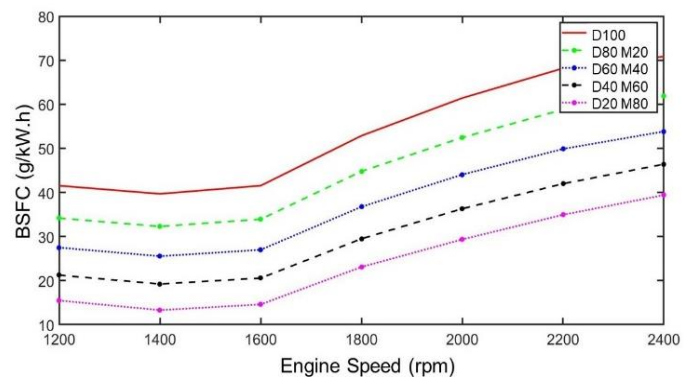


Fig. 13. Specific fuel consumption analysis for different fuel compositions and engine speeds

5.4. Effective efficiency

The effective efficiency results obtained from the theoretical model as a result of adding different proportions of methane to diesel fuel are seen in Figure 14.

Intriguingly, the effective efficiency difference was calculated to be less than 1% at all engine speeds.

When we look at the figure, there are increases in effective efficiency in all methane additions to diesel fuel. The reason for the increases in effective efficiency with the addition of methane is that the lower heating value of the diesel-methane mixture increases due to methane's high lower heating value. As methane's contribution increases, the mixture's total thermal value increases. The increase in power with the increase in the thermal value of the mixture causes an increase in effective efficiency.

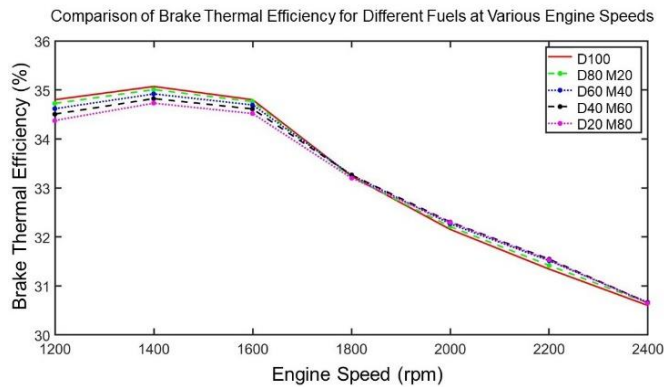


Fig. 14. Effective efficiency for different fuel compositions and engine speeds

5.5. NOx Emissions

The NO_x results obtained from the theoretical model as a result of adding different proportions of methane to diesel fuel are seen in Figure 15. Upon examination, NO_x emissions increase with increasing methane addition. Increases in NO_x emissions occur in all methane additions. The most important effect triggering NO_x emissions is high temperature. The increase in in-cylinder temperature and pressure values with the addition of methane causes an increase in NO_x emissions. Looking at the literature, Ergen stated that the increase in engine load increases in-cylinder temperatures, and this improves combustion characteristics and in-cylinder temperatures, especially dual fuel use, reduces ignition delay and combustion time, and therefore increases NO formation [36]. A. P. Carlucci and others (2008) stated that the use of natural gas addition in diesel engines reduces NO emissions at low engine loads and speeds but increases NO emissions at high engine loads and speeds [37].

The NO_x emissions at 1400 rpm presented significant variance. For instance, a 20% methane input led to a 1.53% difference, resulting in 1477.20 ppm. This trend continued, registering 1496.08 ppm, 1512.80 ppm, and 1527.28 ppm for 40%, 60%, and 80% methane addition.

However, at 2400 rpm, the NO_x emissions changed noticeably. A 20% methane addition revealed a 5.35% disparity, translating to 982.92 ppm. The concentrations rose dramatically, showing 1035.27 ppm, 1085.38 ppm, and 1125.08 ppm for methane levels of 40%, 60%, and 80%.

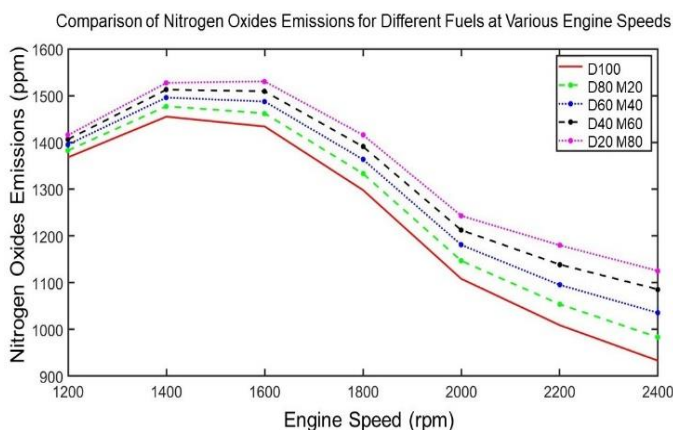


Fig. 15. Comparison of NO_x emissions for different fuel compositions and engine speeds

5.6. CO emissions

Figure 16 illustrates the impact of adding varying amounts of methane to diesel fuel on CO emissions. Upon examining the figure, it becomes apparent that the addition of methane leads to improvements in CO emissions. The reason for the reductions in CO emissions when methane is added to diesel fuel under high loads is that the temperature inside the cylinder increases as the engine load increases. As the temperature inside the cylinder rises, the combustion duration shortens, preventing carbon particles from transforming into CO emissions and slowing down the rate of CO formation, thereby reducing emission values [33,36].

CO emissions at 1400 rpm were also affected by methane levels. With 20% and 40% methane, both had a difference of 5.51% and 10.62%, leading to 0.12%. Interestingly, at 60% and 80% methane levels, the values decreased to 0.11%.

Finally, at 2400 rpm, CO emissions varied slightly. With 20% methane, the difference was only 0.12%, reaching 0.41%. As methane concentration increased to 40%, 60%, and 80%, the values remained close to 0.41%, 0.42%, and 0.42% respectively.

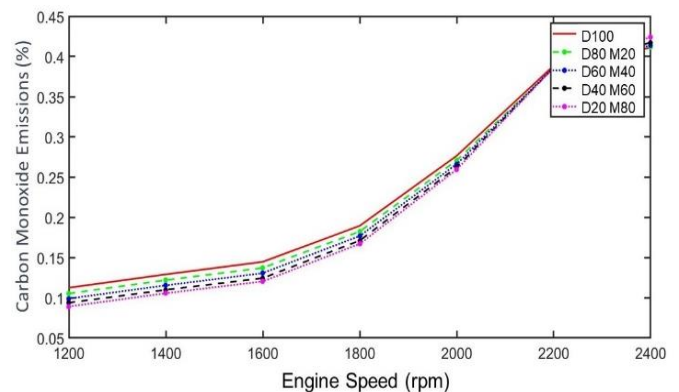


Fig. 16. Comparison of CO Emissions for Different Fuel Compositions and Engine Speeds.

6. Results and Discussion

In this study, a single-cylinder engine model was created in the AVL Boost program using the specific characteristics of the engine and the data obtained from experiments conducted with this engine. The data obtained from the simulation of this single-cylinder engine was compared with the data obtained from the engine experiment, and power, torque, specific fuel consumption, and emission parameters were examined. As a result of this comparison, the percentage difference in values between the experimental data and the data obtained from the simulation is given in Table 5. The reason for the occurrence of percentage errors is that theoretical conditions are considered as perfect situations. These errors can be further reduced with models designed in three dimensions.

Our study elucidated the significant impacts of methane addition to diesel fuel on engine performance. At 1400 rpm, where maximum torque was achieved, a 20% addition of methane notably enhanced the peak pressure by 1.01% to 73.62 bar, and this value further escalated with 80% methane reaching 75.84 bar. However, when the engine was operated at 2400 rpm, indicative of maximum power, peak pressures adopted a divergent trend, peaking at 66.29 bar with 80% methane.

Moreover, the specific fuel consumption at 1400 rpm with a 20% methane infusion demonstrated a 3.09% deviation, and intriguingly, with increased methane proportions, the consumption progressively decreased, showcasing the most efficient value of 213.28 g/kWh at 80% methane addition.

In relation to emissions, NO_x emissions at 1400 rpm with 20% methane surged by 1.53% to 1477.20 ppm, and this ascent became more pronounced at 2400 rpm, culminating in a 5.35% deviation with values soaring to 1125.08 ppm for 80% methane. CO emissions at 1400 rpm, on the other hand, exhibited a reduction at higher methane levels, descending to 0.11% for both 60% and 80% methane additions. However, at 2400 rpm, the variations in CO emissions remained relatively stable across the range of methane concentrations. Notably, throughout our experiments, the effective efficiency showed minimal disparity, remaining under a 1% difference across all engine speeds, underlining the compatibility of methane addition with diesel without severely compromising efficiency.

The research concluded that desired levels of reduction in power and emission values can be achieved by using different methane gas ratios in the correct proportions. Moreover, it was observed that conducting one-dimensional simulations before performing experiments allows for the prediction of experimental results and provides direction for more specific studies. Furthermore, it was proven that the results obtained by integrating numerical calculations with one-dimensional systems show similarity with experimental results, and it was concluded that the accuracy of the models can be increased by adding three-dimensional or two-dimensional studies.

Building on these findings, the integration of theoretical models with experimental data has been demonstrated to be a powerful tool for engine design and optimization. The use of methane as an alternative fuel source, in particular, opens up new avenues for reducing the environmental impact of engine operation. The ability to predict the effects of different methane ratios on engine performance and emissions could lead to more efficient engine designs and fuel usage strategies. Furthermore, the potential to reduce the discrepancy between simulation and experimental data through the use of three-dimensional models offers exciting possibilities for future research. This could lead to even more accurate predictions and a deeper understanding of engine behavior under various operating conditions.

In addition to these findings, it's important to highlight the potential of this research in contributing to the development of more efficient and environmentally friendly engine designs. The use of methane as an alternative fuel, as demonstrated in this study, could significantly reduce the environmental impact of engines, particularly in terms of CO and NO_x emissions. This research also underscores the importance of simulation tools like AVL Boost in predicting engine performance and emissions, thereby reducing the time and cost associated with physical testing. Future work could further refine these models and explore the effects of other alternative fuels, potentially leading to breakthroughs in engine technology and fuel efficiency.

Nomenclature

<i>CH₄</i>	: methane
<i>CO</i>	: carbon monoxide
<i>CO₂</i>	: carbon dioxide
<i>NO_x</i>	: nitrous oxide
<i>LPG</i>	: liquefied petroleum gas
<i>HC</i>	: hydrocarbons
<i>CNG</i>	: compressed natural gas
<i>NiCr</i>	: nickel chrome
<i>CFD</i>	: computational fluid dynamics
<i>EGR</i>	: exhaust gas recirculation
<i>HFK</i>	: air excess coefficient
<i>TDC</i>	: top dead center

Conflict of Interest Statement

The authors declare that there is no conflict of interest in the study.

CRedit Author Statement

Mehmet Fatih Yaşar: Conceptualization, Writing – Original Draft,

Gokhan Ergen: Conceptualization, Validation, Supervision,
Idris Cesur: Conceptualization, Validation, Supervision

References

- [1] Heywood JB. Internal Combustion Engine Fundamentals. McGraw-Hill, New York; 1988. p. 46-48, 417-424, 508-512, 547-552.
- [2] Rodriguez F, Bernard Y, Dornoff J, Mock P. Recommendations for post-Euro 6 standards for light-duty vehicles in the European Union. Communications. 2019;49(30):847102–847129.
- [3] Guerreiro C. Air quality in Europe - 2018 report. Luxembourg: Publications Office of the European Union; 2018.
- [4] World Health Organization. Ambient air pollution: A global assessment of exposure and burden of disease; 2016.
- [5] Richards P. Automotive Fuels Reference Book. Warrendale, PA: SAE International; 2014.
- [6] Papagiannakis RG, Hountalas DT, Rakopoulos CD, Rakopoulos DC. Combustion and Performance Characteristics of a DI Diesel Engine Operating from Low to High Natural Gas Supplement Ratios at Various Operating Conditions. SAE Technical Paper Series. International; 2008. doi: 10.4271/2008-01-1392.
- [7] Liu J, Yang F, Wang H, Ouyang M, Hao S. Effects of pilot fuel quantity on the emissions characteristics of a CNG/diesel dual fuel engine with optimized pilot injection timing. Appl Energy. 2013;110:201–206.
- [8] Imran S, Emberson DR, Diez A, Wen DS, Crookes RJ, Korakianitis T. Natural gas fueled compression ignition engine performance and emissions maps with diesel and {RME} pilot fuels. Appl Energy. 2014;124:354–365.
- [9] Tripathi G, Nag S, Sharma P, Dhar A. Effect of methane supplementation on the performance, vibration, and emissions characteristics of methane-diesel dual fuel engine. Front. Therm. Eng., Sec. Heat Engines. 2023;3.
- [10] Pesyridis A. Effects of Mechanical Turbo Compounding on a Turbocharged Diesel Engine. March 2013 SAE Technical Papers. <https://doi.org/10.4271/2013-01-0103>.

- [11]Tripathi G, Dhar A. Performance, emissions, and combustion characteristics of methane-diesel dual-fuel engines: A review. *Frontiers in Thermal Engineering*. 2022;2. <https://doi.org/10.3389/fther.2022.870077>
- [12]Cubas ALV, Moecke EHS, Ferreira FM, Osório FGS. THC and CO Emissions from Diesel Engines Using Biodiesel Produced from Residual Frying Oil by Non-Thermal Plasma Technology. *Processes*. 2022;10(8):1663.
- [13]Wojs MK, Orliński P, Kruczyński SW. Combustion process in dual fuel engine powered by methane and dose of diesel fuel. *Zeszyty Naukowe Instytutu Pojazdów/Politechnika Warszawska*. 2016;1/105:61–68.
- [14]Stravinskas S, Rimkus A, Kriaučiūnas D. Analysis of the Combustion Process of a Compression Ignition Engine Running on Diesel and Natural Gas. *Transportation Science and Technology*. Springer International Publishing; 2020. pp. 591–600.
- [15]Papagiannakis RG, Hountalas DT. Combustion and Exhaust Emission Characteristics of a Dual Fuel Compression Ignition Engine Operated with Pilot Diesel Fuel and Natural Gas. *Energy Conversion and Management*. 2004;45:2971–2987.
- [16]Nwafor OMI. Effect of Choice of Pilot Fuel on The Performance of Natural Gas in Diesel Engines. *Renewable Energy*. 2000;21:495–504.
- [17]Abd-Alla GH, Soliman HA, Badr OA, Abd-Rabbo MF. Effect of Injection Timing on The Performance of a Dual Fuel Engine. *Energy Conversion and Management*. 2002;43:269-277.
- [18]Shi Y, Ge HW, Reitz RD. *Computational Optimization of Internal Combustion Engines*. London: Springer London; 2011. doi: 10.1007/978-0-85729-619-1.
- [19]Çaylar G. The Effect of Ethanol Addition to Fuel on Engine Emission and Performance in Internal Combustion Engines. Master Thesis, Department of Mechanical Engineering, Institute of Science and Technology, Istanbul Technical University; Istanbul, Turkey; 2018.
- [20]Badra JA, Khaled F, Tang M, Pei Y, Kodaseval J, Pal P, Mattia B, Aamir F. Engine Combustion System Optimization Using Computational Fluid Dynamics and Machine Learning: A Methodological Approach. *J Energy Resour Technol*. 2021;143(2).
- [21]Woschni G. A Universally Applicable Equation for the Instantaneous Heat Transfer Coefficient in the Internal Combustion Engine. *SAE Technical Paper Series*. 1967;1.
- [22]Cerdoun M, Carcasci C, Ghenaïet A. Analysis of unsteady heat transfer of internal combustion engines' exhaust valves. *International Journal of Engine Research*. 2019;19(6):613–630.
- [23]Zapf H. Beitrag zur Untersuchung des Wärmeübergangs während des Ladungswechsels im Viertakt-Dieselmotor. *MTZ*. 2017;30(12):461–465.
- [24]Chmela FG, Orthaber GC. Rate of heat release prediction for direct injection diesel engines based on purely mixing controlled combustion. *SAE Technical Papers*. 1999;108:152–160.
- [25]Pattas K, Häfner G. Stickoxidbildung bei der ottomotorischen Verbrennung. *MOTORMemo*. 1973;34(12).
- [26]Onorati A, Ferrari G, D'Errico G. 1D Unsteady Flows with Chemical Reactions in the Exhaust Duct-System of S.I. Engines: Predictions and Experiments. 2001. doi: 10.4271/2001-01-0939.
- [27]Sürmen A, Karamangil MA, Arslan R. Motor termodinamiği. *Aktüel Yayınları*; 2004.
- [28]Hardenberg HO, Hase FW. An empirical formula for computing the pressure rise delay of a fuel from its cetane number and from the relevant parameters of direct-injection diesel engines. *SAE Technical Papers*. 1979;1823–1834.
- [29]Wiebe J. Progress in engine cycle analysis: Combustion rate and cycle processes. *Mashgiz, Ural-Siberia Branch*; 1962. 271.
- [30]Ghojel JI. Review of the development and applications of the Wiebe function: A tribute to the contribution of Ivan Wiebe to engine research. *International Journal of Engine Research*. 2010;11(4):297–312.
- [31]Henein NA, Bolt A. Ignition Delay in Diesel Engines. *SAE Transactions*. 1968;76(1):27-49.
- [32]Boerlage GD, Van Dyck WCD. Causes of Detonation in Petrol and Diesel Engines. *Proceedings of the Institution of Automobile Engineers*. 1974;28(2):366–409.
- [33]Ergeneman M, Mutlu M, Kutlar OA, Arslan H. *Exhaust Pollutants from Vehicles*. Birsen Publishing House; Istanbul; 1998. 1–14.
- [34]Mansor MRA, Abbood MM, Mohamad TI. The influence of varying hydrogen-methane-diesel mixture ratio on the combustion characteristics and emissions of a direct injection diesel engine. *Fuel*. 2017;190:281–291.
- [35]Vávra J, Bortel I, Takáts M, Diviš M. Emissions and performance of diesel natural gas dual-fuel engine operated with stoichiometric mixture. *Fuel*. 2017;208:722–733.
- [36]Ergen G. The Effects of Biofuel and Additive Usage on Partial Load Performance and Emission Characteristics in a Dual Fuel Diesel Engine Using Natural Gas. PhD Thesis, Sakarya University; 2011.
- [37]Carlucci P, Risi AD, Laforgia D, Naccarato F. Experimental investigation and combustion analysis of a direct injection dual-fuel diesel–natural gas engine. *Energy*. 2008;33(2):256–263